International Journal of Transportation Engineering and Technology
2016; 2(4): 42-48
http://www.sciencepublishinggroup.com j/ijtet
doi: 10.11648/j.ijtet.20160204.12

Hybrid Propulsion Testing using Direct-Drive Electrical Machines for Super Yacht and Inland Shipping

Johannes J. H. Paulides[1, 2], Nenad Djukic[1, 2], Johannes A. de Roon[1], Laurentiu Encica[1]

[1]Advanced Electromagnetics BV, Sprang-Capelle, The Netherlands

[2]Electromechanics and Power Electronics, Eindhoven University of Technology, Eindhoven, The Netherlands

Email address:

johan@ae-magnetics.nl (J. J. H. Paulides), j.j.h.paulides@tue.nl (J. J. H. Paulides)

To cite this article:

Johannes J. H. Paulides, Nenad Djukic, Johannes A. de Roon, Laurentiu Encica. Hybrid Propulsion Testing using Direct-Drive Electrical Machines for Super Yacht and Inland Shipping. *International Journal of Transportation Engineering and Technology*. Vol. 2, No. 4, 2016, pp. 42-48. doi: 10.11648/j.ijtet.20160204.12

Received: August 31, 2016; **Accepted**: October 31, 2016; **Published**: November 25, 2016

Abstract: Hybrid or full electric propulsions for inland ships are becoming more popular. In these application, direct-drive PM propulsion motors are a preferred machine configuration. This paper discusses the challenges to determine the losses, as estimated with simulations, during the testing procedures of a 350kW at 300rpm, respectively. The full-load testing of the drive system is performed by mechanically coupling two identical machines, of which one operates as a motor and the other as a generator, or "back-to-back" testing configuration. Two Direct-Drive PM machines have been manufactured to validate key findings from the modelling, particularly in terms of loss predictions, thermal modelling and influence of the design features such as magnet segmentation. A back-to-back set-up is created for testing these machines with a speed range of 0-450 rpm. Before the measurement commended, tests were carried out in accordance with IEC60034-1, IEC60034-15, IEC60085-1, IEEE43, IEEE118 and Lloyd's register. These tests included: surge, resistance, winding symmetry, high voltage test, insulation resistance and polarization index. All these tests were successfully completed and agreed with the analysis as described before. Following the motors have been installed in an inland ship hybrid propulsion.

Keywords: Hybrid Propulsion, High Torque Machines, Electric Vessel, Hybrid Ship, Super Yacht, Hybrid Yacht, Brushless Machine, Electric Propulsion, Electrical Machines, Testing, Direct-Drive Motor

1. Introduction

DIESEL-ELECTRIC propulsion is very effective in ships that are operated in partial load conditions for a significant portion of their time, e.g. inland ships that require up-, down-stream, harbor and canal operation. The main advantages of the diesel-electric propulsion are: flexibility (better space utilization and redundancy), more economical operation, less maintenance and reduced environmental pollution. In these hybrid ships, the popularity of diesel-electric propulsion systems (0.5–3.0 MW range) is ever increasing, since potentially 10-25% diesel fuel can be saved on specific journeys [1, 2]. Of course, also in shipping applications operating costs should be minimized, hence it is no surprise that fleet owners are considering high-efficient machines that can directly drive their propeller for their diesel-electric propulsion [3, 4]. Of course, there are different hybrid topologies requiring sizing criteria of components and related control strategies, finalized to maximize different objective functions: weight and space reduction on-board, fuel economy, pollution reduction or optimized efficiencies [5].

This paper concerns the testing of electrical machines for a hybrid propulsion for an inland ship application. Some authors have also described such high torque PM motors which are special to this system, including the use of 16-phase windings for lower harmonic content, larger damper winding arrangements and high strength rotor magnet containment [6]. While others have reviewed DC hybrid systems by modeling and simulation [7]. Further, the high level of complexity of hybrid systems is also giving rise to modern sophisticated ship electrical power management and control systems resembling the ones adopted in land-based hybrid systems [8]. Beside in-land ship applications, hybrid propulsion is also considered for luxury yacht applications [9]. Modeling is an important aspect of these hybrid systems as also discussed in [10]. In general modeling of electrical machines is an important aspect to advance electrical

machines [11-15]. This is also the subject of this paper, where these models are aided by tests that are challenging in nature.

Fig. 1. *Statendam I and II, a double propeller inland vessel with a hybrid propulsion system.*

2. Hybrid Ship Propulsion Solutions

Most inland ships today are equipped with a traditional propulsion systems based on an internal combustion engine (ICE). However, new ways are continuously introduced to conceive propulsion and power systems for inland shipping. Within these propulsion solutions, medium-speed diesel or gas engines (variable speed ICE's) are connected to the propeller through a reduction gear. Considering transmission losses means that for the same propeller power, medium speed diesel engines must develop about 2-5 percent more power in the geared design at full load [16]. However, at partial load considerably more losses are present.

A "hybrid propulsion" (Fig. 1) is considered a propulsion where a geared ICE (medium-speed engine is connected to the propeller by a transmission and shaft) is combined with a high torque electric machine, i.e. a parallel hybrid solution [17].

This parallel hybrid, Fig. 2, allows for three modes:

1. *Electric cruise mode;* at low speed, hence low power (<250kW) the boat is driven by the electric machine. Diesel-electric generator sets and/or battery pack are used to provide the energy for this electric cruising.
2. *Generator mode;* the propulsion is provided by the diesel engine s) and the hotel load is supplied and/or on-board battery pack is charged. This allows one or two engine-generator groups (or generator sets) to be switched off, since enough power can be generated in generator mode.
3. *Boost mode;* the high speed and high power (<350kW) range uses the Boost mode to support the combustion engine with the constant torque of the electric motor. Also an improved response of the propulsion occurs through the boost mode.

The resulting fuel efficiency depends on many variables, e.g. ship type (length, width, hull profile, etc.), trajectory (river, canals, depth, etc.) and load-cycle (frequency and magnitude of accelerations, duration of the stops, distances to be covered, etc.). Although that on average a hybrid propulsion always improves fuel efficiency due to the smaller main diesel that can be installed. Considering the inland application, for some specific journeys fuel savings can even be 25% [18].

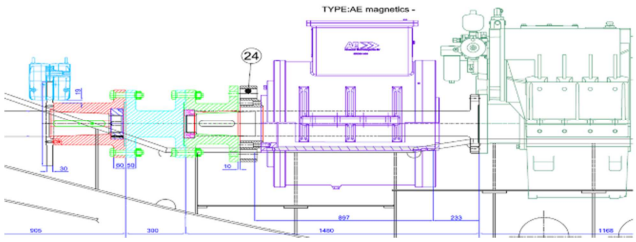

Fig. 2. *Propulsion schematic hybrid ship [8].*

3. Electromagnetic Design

Although specific electric machines can reach power density in the range of 6-12 kW/kg [19, 20], this coincides with high speed operation. The electric motor (0-336rpm) is directly coupled to the propulsion shaft, hence around 0.2 kW/kg or 7 Nm/kg (using total mass of machine, including bearings, etc.) can be achieved. The line current, line-line EMF and instantaneous torque are calculated using an analytical method (PC-BDC v10.02 [21]), where the finite-element analysis results are displayed in Fig. 3 It needs noting that this finite element analysis assumes the stator current waveform to be ideally sinusoidal.

3.1. Stator Copper Losses

An initial estimate of the copper loss at rated current for a machine design of a given packing factor can be derived from the geometrical considerations of the winding:

$$P_{CU} = 3 \cdot I_{ph,rms}^2 \cdot R_{ph} = 3 \frac{J^2 Vol_{cu}}{\sigma_{cu}} \quad (1)$$

where R_{ph} is the phase resistance, J is the current density, Vol_{cu} is the volume of copper and σ_{cu} is the conductivity of copper. For this machine design, the total copper loss is 12.9kW at a 130°C temperature increase.

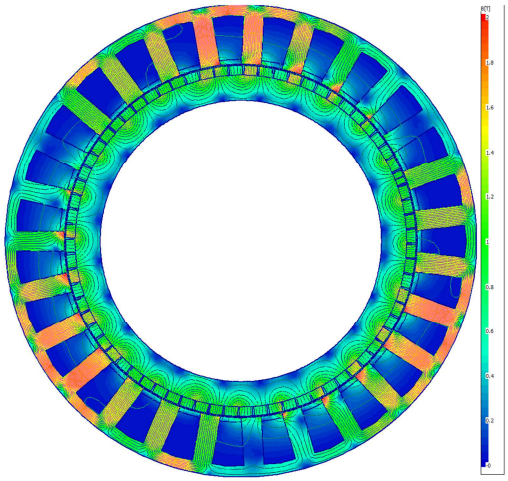

Fig. 3. *Full-load finite element analysis result.*

3.2. Stator Iron Losses

The low-speed nature of this application is likely to mean that stator iron loss will constitute a small proportion of the total loss. Here, the iron losses are obtained using finite-element computations. This calculation assumes sinusoidal currents, i.e. no switching frequency effect, and therefore the total losses are expected to be somewhat higher than estimated (~1.5-2 times). This gives that for a standard grade of 0.5mm lamination around 2.5kW iron loss is estimated.

3.3. Magnet Losses

A critical design issue in water cooled PM machines is magnet loss. A number of design features are often incorporated into permanent magnet rotors to reduce the rotor magnet losses: rotor magnet segmentation, electrically conducting rotor screens and alternative winding configurations and phase numbers [22-24]. Here, the full-load loss has been analyzed using transient finite element analysis coupled to an electrical circuit. The electrical circuit consists of a three-phase inverter. The eddy-current skin depth within the magnets is 70.9mm, which is much larger than the magnet thickness (14mm), meaning the eddy-current are resistance limited and have been estimated via analytical methods to be ~600W at 300rpm, respectively.

4. Thermal Design

Accurate thermal modelling is critical to ensure that a design is viable in terms of the maximum temperature constraints. A lumped parameter equivalent thermal network approach was adopted using Motor-CAD [25], as shown in Fig. 4. This model employs an equivalent thermal network consisting of power sources, thermal resistances and thermal capacitances. In this model a total copper loss of 480W is generated in the region of the coil shown (this value corresponding to a rated load overall copper loss of ~13kW for the entire machine, which consist of 27 such half coil regions).

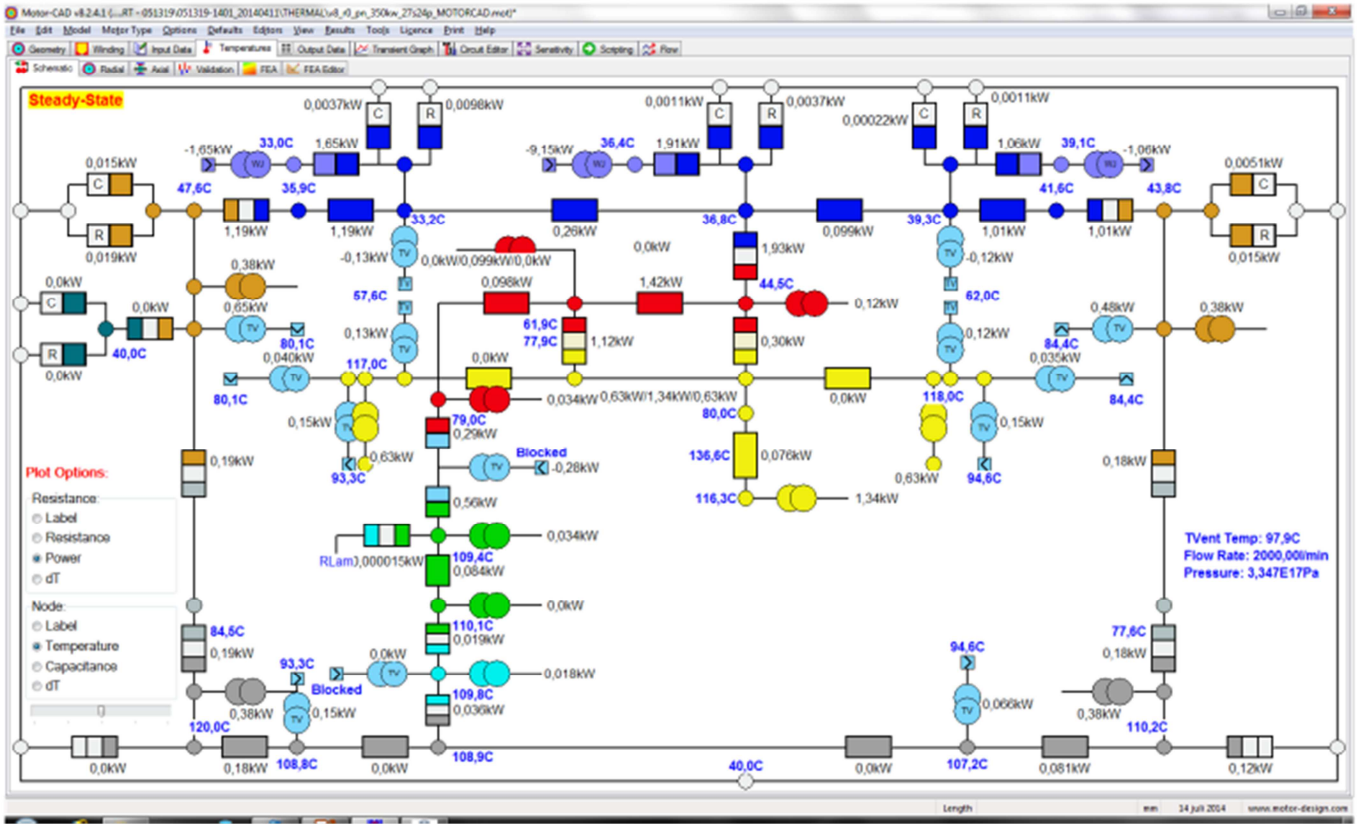

Fig. 4. *Used lumped parameter model illustrating the various temperatures within the machine.*

5. Motor Manufacturing & Testing

Two PM machines have been manufactured to experimentally validate the design procedure employed. The objectives of this experimental phase are to validate key findings from the modelling, particularly in terms of loss predictions, thermal modelling and influence of the design features such as magnet segmentation. A back-to-back set-up is created for testing this machine with a continuous power rating of 0-350kW, with a speed range of 0-400 rpm. Before the measurement commended, tests were carried out in accordance with IEC60034-1, IEC60034-15, IEC60085-1, IEEE43, IEEE118 and Lloyd's register. These tests included: resistance measurement, winding symmetry, high voltage test, insulation resistance, polarization index and surge test. All these tests were successfully completed and agreed with the analysis as described before.

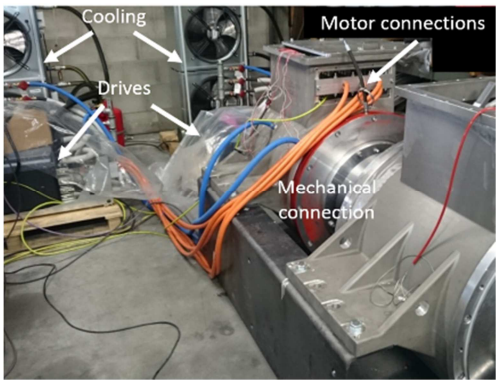

Fig. 5. Back-to-back test set-up illustrating drives and cooling.

The full-load testing of the drive system is performed by mechanically coupling two identical machines, as shown in Fig. 5. This arrangement is considered a "back-to-back" testing configuration. The power is supplied by two inverters supplying the motor and the generator, where the losses are supplied to one of the inverters from the grid (or a diesel genset that is not in the picture). Finally, the generator feeds the inverters that return the power via the DC-link back to the inverter of the motor. From an overall power balance, it is clear that most of the power involved in the test flows in a closed loop, while the grid or diesel genset supplies only a power equal to the total losses of the system under test.

The most significant results of the back-to-back testing are to confirm the modelling approach. The next test have been performed:

5.1. Assessment of Motor Thermal Performance by Supplying Almost Pure Reactive Power from the Inverter

A heat-run test is performed to assess the thermal behavior for 150kVar and 320Arms. During the heat-run test, the temperature inside the motor is monitored by means of various Pt100 thermal sensors, some of which are embedded in stator slots, others are fixed on end coils and placed in close proximity to the bearings. The results obtained for the winding are shown in Fig. 6. This has confirmed the thermal analysis as has been reported before.

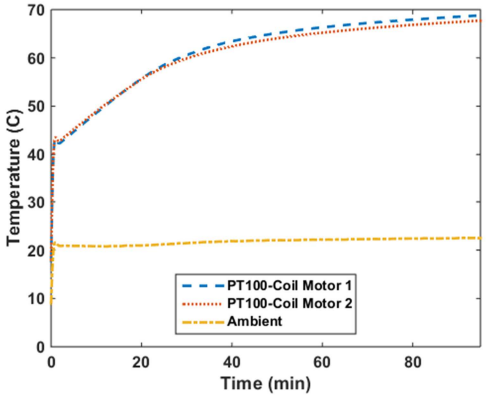

Fig. 6. Winding temperature with scalar control (150kVar and 320A).

5.2. Assessment of No-load Losses Within the Motor

This closed-loop test has been carried out at 200rpm. Fig. 7 illustrates the results, where input active power, reactive power, power factor and speed have been recorded. Both motors where linked and then tested for no load power loss. The temperature ranged between 30 and 40dC. If the back-to-back test set-up was run by Motor 1, a power usage of 6.5kW and 7.6kVar at 200rpm was measured. Checking this input power by running the set-up from motor 2 resulted in a power requirement of 6.8 kW and 8.4 kVar. This small difference of 300W has been identified as variation in bearing losses or temperature effects. The total input power of around 6.6kW that was required for this test comprises of variation in winding resistance, bearing, magnet, windage and no-load iron losses.

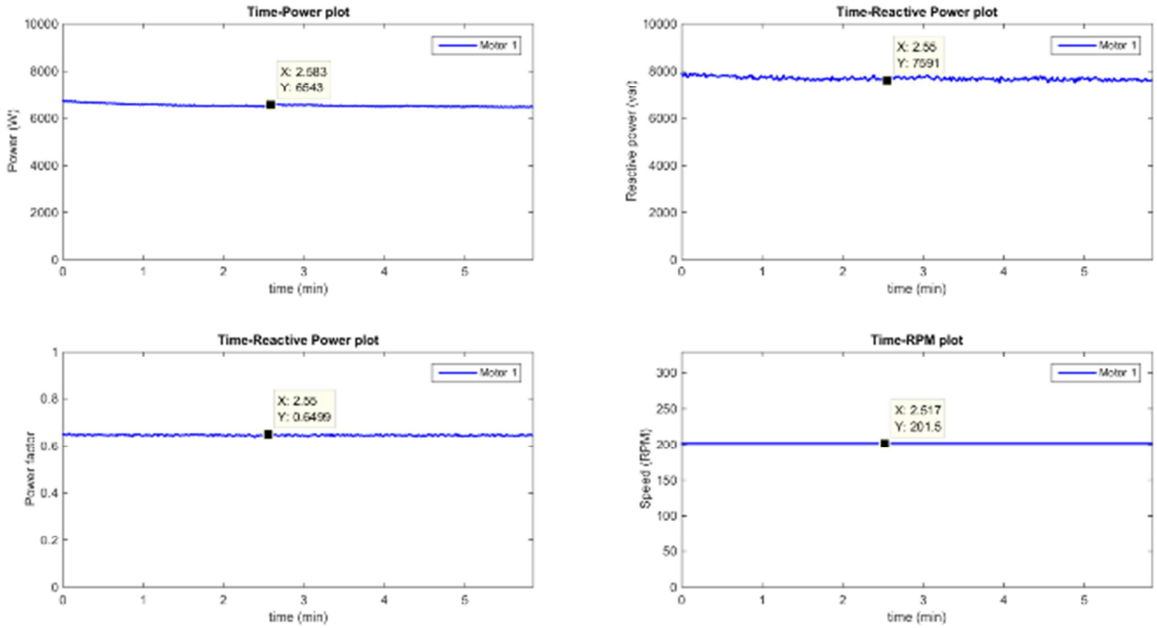

Fig. 7. Test (3) results, illustrating no-load input power in the back-to-back configuration.

5.3. Assessment of the Rated Motor Torque

The motor shall be capable of supplying the torque corresponding to 11,000Nm at 100rpm (motor is dominated by copper loss and half to full speed iron loss increase is considered to be small). The result of the test is summarized in Fig. 8, which shows motor input power, generator output power, mechanical power on the shaft, and efficiency and temperatures of motor and generator both during the test.

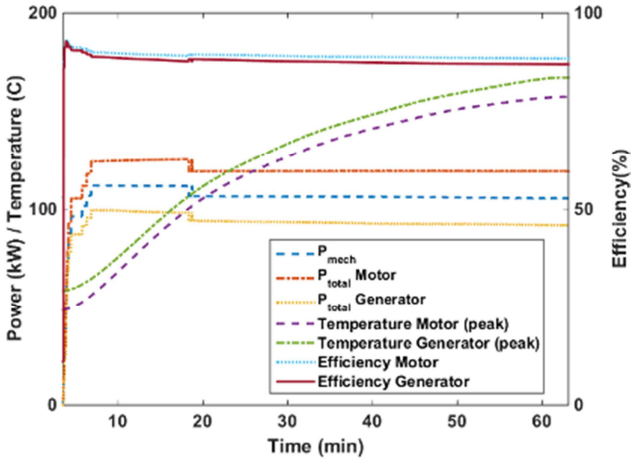

Fig. 8. *Test (4), full load results illustrating shaft power, input motor power, output generator power, peak winding temperature and efficiency.*

The temperature in Fig. 8 is the peak winding temperature as recorded during the tests. However, following the measurement the average temperature was recorded using the winding resistance. Consequently Fig. 8 has been updated to represent the average temperature of the stator winding, as shown in Fig. 9. Further, this illustrates the copper losses and the remaining losses as extracted from the measurements. Initially a higher torque set point was given to the back-to-back test to shorten the total testing time by reducing the transient temperature rise during the test.

5.4. Assessment of Torque Versus Current Dependency

From electrical measurements, i.e. computing the ratio between the total instantaneous electrical power measured at motor terminals and the speed acquired through a dedicated encoder, an estimation is obtained of the "air gap" or "electromagnetic" torque. Here, the motor has to supply more torque compared to the generator. This torque contains some high frequency torque components due to converter switching. Although that these components are mechanically damped while being transferred from the air gap to the shaft through the solid-steel rotor body. Fig. 10 shows the resulting estimated shaft torque which satisfies the initial design target.

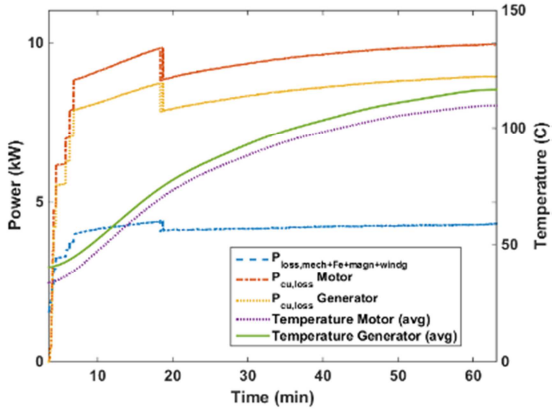

Fig. 9. *Test (4), full load results illustrating estimation of copper loss and remaining losses and average winding temperature.*

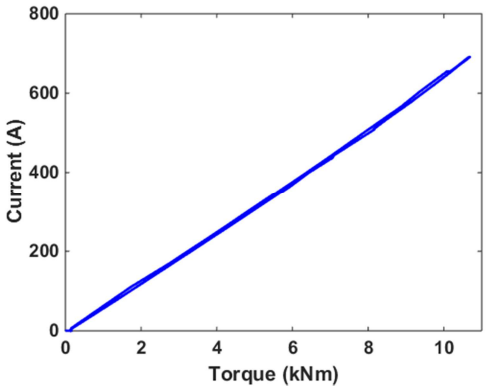

Fig. 10. *Assessment of Torque versus Current dependency.*

After successful completion of mechanical and electrical commissioning activities, the actual motors where delivered to the customer, as shown in Fig. 11. The performance exhibited and the hours of reliable operation achieved so far demonstrated the validity of the technologies and design strategies employed for both single components of the system and their integration.

6. Conclusion

Direct-drive PM electric machines on the propulsion shaft of advanced hybrid propulsion allows ship-owners to take advantage of a more flexible, modular, efficient and lightweight propulsion system. This paper reports on back-to-back testing that can be applied when two or more electrical machines of the same type are produced. The main advantages of this kind of electrical machine testing are:

- no driving machine is needed for the testing; the role of driving machine is given to one of the tested machines;
- possibility of testing two newly produced machines at the same time;
- recuperation of the energy; only total losses have to be supplied form the grid or other source;

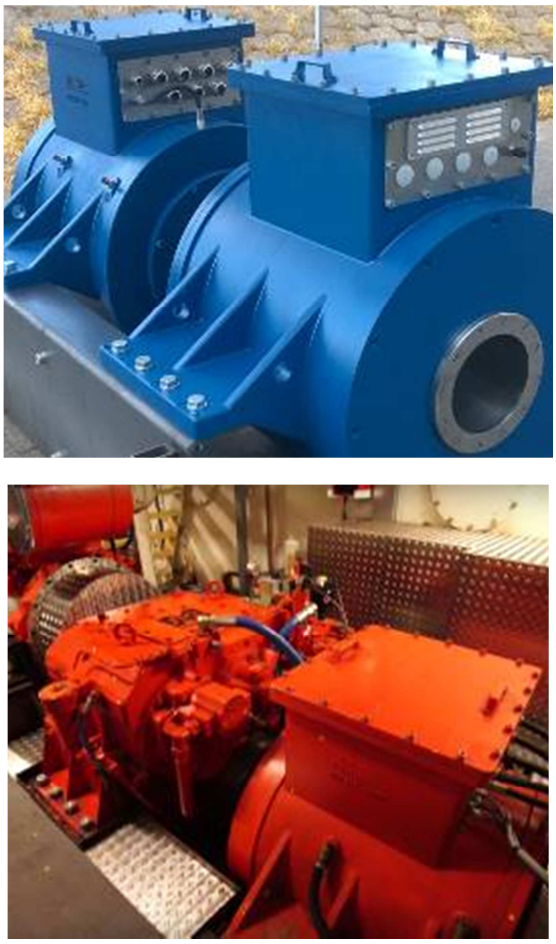

Fig. 11. *Finalized motors as delivered for the hybrid shipping application.*

References

[1] The next generation of ECO SHIP, (2002) "The Development of an electric propulsion domestic chemical tanker, http://www.nakatani-sy.co.jp/index_er.html

[2] G. J. de Gelder, (2014) "10-15% fuel saving", http://www.groenervaren.nl/tweede-hybride-binnenvaartschip/

[3] J. M. Apsley, A. Gonzalez-Villasenor, M. Barnes, A. C. Smith, S. Williamson, J. D. Schuddebeurs, P. J. Norman, C. D. Booth, G. M. Burt, and J. R. McDonald (2009) "Propulsion drive models for full electric marine propulsion systems," IEEE Trans. Ind. Appl., vol. 45, no. 2, pp. 676-684.

[4] R. E. Hebner (2005) "Electric ship power system-Research at the University of Texas at Austin," in Proc. IEEE Electric Ship Technol. Symp., Jul. 25-27, pp. 34-38.

[5] A. Del Pizzo, R. M. Polito, R. Rizzo, P. Tricoli (2010) "Design Criteria of On-board Propulsion for Hybrid Electric Boats", XIX International Conference on Electrical Machines - ICEM 2010, Rome, pp. 1-6.

[6] S. Kuznetsov (2011) "Machine design and configuration of a 7000 hp hybrid electric drive for naval ship propulsion", IEEE International Electric Machines & Drives Conference (IEMDC), pp. 1-4.

[7] B. Zahedi, and Lars E. Norum (2013) "Modeling and simulation of all-electric ships with low-voltage DC hybrid power systems", IEEE Trans. on Power Electronics, Vol. 28, No. 10, pp. 4525-4537.

[8] C. Patsios, G. Antonopoulos and J. Prousalidis (2012) "Discussion on adopting intelligent power management and control techniques in integrated power systems of all-electric ships", Electrical Systems for Aircraft, Railway and Ship Propulsion (ESARS), pp. 1-6.

[9] D. Bosich, G. Sulligoi (2013) "Voltage control on a refitted luxury yacht using hybrid electric propulsion and LVDC distribution", Eighth International Conference and Exhibition on Ecological Vehicles and Renewable Energies (EVER), pp. 1-6.

[10] T. Jaster, A. Rowe and Z. Dong (2014) "Modeling and simulation of a hybrid electric propulsion system of a green ship", IEEE/ASME 10th International Conference on Mechatronic and Embedded Systems and Applications (MESA), pp. 1-6.

[11] S. Jumayev, J. J. H. Paulides, K. Boynov, J. Pyrhonen, & E. A. Lomonova (2016) "Three-dimensional analytical model of helical winding PM machines including rotor eddy-currents", IEEE Transactions on Magnetics, Vol. 52, Issue 5, pp. 1-12

[12] R. L. J. Sprangers, J. J. H. Paulides, B. L. J. Gysen, & E. A. Lomonova (2016). Magnetic saturation in semi-analytical harmonic modeling for electric machine analysis. IEEE Transactions on Magnetics, Vol. 52, Issue 2, pp. 1-10.

[13] J. Jacob, J. A. Colin, H. Montemayor, D. Sepac, H. D. Trinh, S. F. Voorderhake, P. Zidkova, J. J. H. Paulides, A. Borisavljevic, & E. A. Lomonova (2015) "InMotion hybrid racecar: F1 performance with LeMans endurance". COMPEL: The International Journal for Computation and Mathematics in Electrical and Electronic Engineering, 34 (1), pp. 210-233.

[14] M. F. J. Kremers, J. J. H. Paulides & E. A. Lomonova (2015) "Towards accurate design of a transverse Flux machine using an analytical 3-D magnetic charge model", IEEE Transactions on Magnetics, Vol. 51, Issue 11, pp. 1-4

[15] R. L. J. Sprangers, J. J. H. Paulides, B. L. J. Gysen, J. Waarma, & E. A. Lomonova (2015) "Semi-analytical framework for synchronous reluctance motor analysis including finite soft-magnetic material permeability", IEEE Transactions on Magnetics, Vol. 51, Issue 11, pp. 1-12

[16] R. Whitney, (2013) "Ship Energy Efficiency Measures Advisory", ABS Houston USA, pp.1-72.

[17] J. J. H. Paulides, N. Djukic, & L. Encica (2015) "Hybrid shipping for inland navigation: Loss analysis of an aluminum direct-drive high performance 11,000Nm Permanent Magnet machine", (EVER 2015), 31 March - 2 April 2015, Monte Carlo, Monaco, (pp. 1-5)

[18] C. D. Christophel (2011) "Reduzierung der CO2-Emissionen durch diesel-elektrische Antriebe am Beispiel eines bestehenden Motorgüterschiffes", Workshop CO2-Emissionen der Binnenschifffahrt, pp. 1-11.

[19] Electric Marine Support Binnenvaart B. V. (2015) "Ship schematic for Hybrid Ship", www.electricmarinesupport.nl/.

[20] S. Kuznetsov (2011) "Machine design and configuration of a 7000 HP hybrid electric drive for naval ship propulsion", IEEE International IEMDC, pp. 1625-1628.

[21] J. J. H. Paulides, L. Encica, T. F. Beerneart, H. H. F van der Velden, A. G. P. Parfant and E. A. Lomonova, "Ultra-light-weight high torque density brushless PM machine design: Driving-cycle investigation of a Four-Wheel drive race car", 2015 Tenth International Conference on Ecological Vehicles and Renewable Energies (EVER), pp. 1-7.

[22] "SPEED," available on http://www.cd-adapco.com.

[23] N. Taghizadeh Irenji, S. M. Abu Sharkh, M.R. Harris (2000) "Effect of rotor sleeve conductivity on rotor eddy-current loss in high-speed PM machines", ICEM Espoo Finland, pp. 645-648.

[24] J. L. F. Van der Veen, L. J. J. Offringa, A. J. A. Vandenput (1997) "Minimising rotor losses in high-speed high-power permanent magnet synchronous generators with rectifier load", IEE Proc Electrical Power applications, Vol. 144, No. 5, pp. 331-337.

[25] E. Bunzel, G. Mueller (1991) "General analysis of a 6-phase synchronous machine", Int. conf. Evolution and modern aspects of synchronous machines, pp. 333-340.

[26] "Motor-CAD and Motor-LAB," available on www.motor-design.com.